Journal of Flow Control, Measurement & Visualization, 2022, 10, 87-97
https://www.scirp.org/journal/jfcmv
ISSN Online: 2329-3330
ISSN Print: 2329-3322

# Quantitative Visualization of Two-Phase Acoustic Streaming Emitted from Ultrasonic Scaler

**Takayuki Yamagata[1], Kota Kato[1], Naoki Takahashi[2], Syuhei Mineo[2], Koichi Tabeta[2]**

[1]Graduate School of Science and Technology, Niigata University, Niigata, Japan
[2]Graduate School of Medical and Dental Sciences, Niigata University, Niigata, Japan
Email: yamagata@eng.niigata-u.ac.jp

**How to cite this paper:** Yamagata, T., Kato, K., Takahashi, N., Mineo, S. and Tabeta, K. (2022) Quantitative Visualization of Two-Phase Acoustic Streaming Emitted from Ultrasonic Scaler. *Journal of Flow Control, Measurement & Visualization*, **10**, 87-97.
https://doi.org/10.4236/jfcmv.2022.103006

**Received:** February 11, 2022
**Accepted:** March 14, 2022
**Published:** July 8, 2022



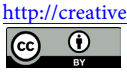



## Abstract

This study experimentally investigated two-phase acoustic streaming and droplet properties of aerosols, which were generated by a dental ultrasonic scaler. The velocity field of acoustic streaming was measured using particle image velocimetry with the generated liquid droplets as tracers, and the shadowgraph technique was adopted to measure the droplet diameter. In the PIV measurement of the gas-liquid two-phase flow, the injection of oil smoke substantially suppressed the number of invalid vectors. The acoustic streaming of the ultrasonic scaler showed maximum velocity at a region away from the scaler tip, and the maximum velocity increased with an increase in the liquid flow rate. The droplets of the ultrasonic scaler were generated by capillary waves and had a diameter on the order of tens of micrometers. These droplets effectively enhanced the velocity of the acoustic streaming in the two-phase case compared to the single-phase case without the droplets.

## Keywords

Acoustic Streaming, Ultrasonic Scaler, Aerosol, Particle Image Velocimetry, Shadowgraph Method

## 1. Introduction

In recent years, measures to prevent the spread of COVID-19 have been implemented in various fields. In dental industry, the risk of cross-infection caused by aerosols resulting from the use of the ultrasonic scaler on treatment instruments is a major concern [1]. Aerosols are generated by the atomization of the cooling water for the ultrasonic scaler and transported by acoustic streaming.

Liquid atomization is important for many industrial processes, such as spray drying, film coating, and liquid fuel combustion. Most industrial applications require methods for atomizing a narrow droplet size distribution. Therefore, researchers have attempted to predict the average droplet diameter based on the capillary wave theory [2], and investigated the effects of liquid phase properties [3], operating frequency, and power dissipation [4] on the droplet size distribution. However, information on the droplet velocity generated by ultrasonic atomization is insufficient.

Acoustic streaming is a phenomenon in which a part of the sound energy is dissipated by the fluid viscosity, resulting in a net mean flow [5]. The acoustic streaming generated from the ultrasonic scaler is an Eckart-type streaming, which is characterized by a considerably larger vortex scale than that of the acoustic wavelength [6]. This type of acoustic streaming has been investigated in the field of fluid mixing [7] [8], flow control [9] [10], and sonochemistry [11]. The induced velocity fields were measured by quantitative flow visualization using particle image velocimetry (PIV) [12] [13] [14]. These studies revealed that an ultrasonic transducer induced a jet motion similar to that of a turbulent free jet with the maximum velocity occurring at a position different from the acoustic focus. The maximum velocity and position are affected by the tip shape of the ultrasonic transducer [15]. Furthermore, microbubbles in water increase the rate of absorption of the acoustic energy and accelerate acoustic streaming [16]. Although studies on the basic structure of ultrasonic acoustic streaming have been conducted, they have mainly focused on acoustic streaming in single-phase flows. Therefore, there are few reports on acoustic streaming under gas–liquid two-phase flow conditions, such as those of ultrasonic-scaler-induced aerosols.

The objective of this study was to investigate the two-phase acoustic streaming characteristics and droplet properties generated by a dental ultrasonic scaler.

## 2. Experimental Methods

A dental ultrasonic scaler (Suprasson P-MAX) was used for the experiments. **Figure 1** shows a photograph of the standard-shaped scaler tip used in this study. The tip had a diameter of approximately 2 mm and was curved into a bow-shape. The bisector of the curved scaler tip was defined as the horizontal direction ($x$) in this study. The cooling water was supplied with a peristaltic pump from the bowed part. The oscillation frequency of the ultrasonic scaler was 30 kHz, and the output power and flow rate of the cooling water were variable.

Velocity field measurements using PIV were performed to clarify the characteristics of the air-water two-phase acoustic streaming from an ultrasonic scaler. **Figure 2(a)** shows a schematic of the PIV measurements. The PIV system consisted of a CMOS camera (IDT, MotionPro-Y4, 1024 × 1024 pixels with 8 bits), Nd: YAG pulsed laser (Quantel, EverGreen, 70 mJ/pulse), and pulse generator. The liquid droplet generated from the ultrasonic scaler was used as a tracer for

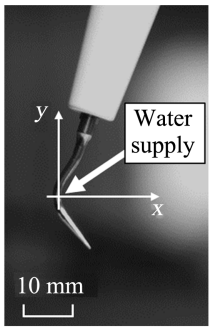


**Figure 1.** Ultrasonic scaler tip.

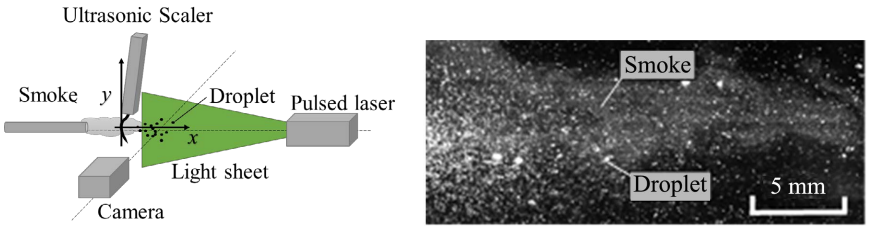


(a) (b)

**Figure 2.** Schematic of the PIV system. (a) Experimental setup;(b) Representative image.

the PIV. Oil smoke particles were supplied from behind the ultrasonic scaler tip as the particle number density required for suitable PIV analysis could not be obtained (see **Figure 2(b)**). The oil smoke was generated by a heated fog machine and blown through a tube with a diameter of 10 mm. The diameter of the smoke particles was approximately 1 μm. The speed of the oil smoke particles was sufficiently slow compared to the target flow, which was less than 5% of the maximum speed. The addition of smoke tracers reduced the average rate of invalid vectors from 4.1% to 2.9%. The target area of the velocity measurement was determined to be a vertical cross-section where the major acoustic streaming was confirmed by visual observation. PIV measurements were conducted with an imaging area of 40 mm × 40 mm and a recording period of 0.1 s. The velocity field was evaluated using a direct cross-correlation algorithm with a sub-pixel interpolation of the Gaussian peak-fitting technique [17]. The interrogation window size was 31 × 31 pixels, with a 50% overlap. The time interval between two consecutive images was $\Delta t$ = 60 - 600 μs, depending on the target flow velocity. The maximum displacement of the particles was approximately five pixels under these conditions. The uncertainty of the PIV measurement was estimated to be 2.7% using the uncertainty quantification [18]. The average velocity field was obtained from 500 instantaneous datasets. The PIV experiment was performed under the conditions that the output power was 4, 6, 8, and 10 out of 10, and the liquid flow rates were 0, 0.07, 0.14, and 0.38 ml /s.

The liquid droplet properties in the aerosol generated by the ultrasonic scaler were evaluated using the shadowgraph method. **Figure 3(a)** shows a schematic of the experimental setup. The CMOS camera was used for the shadowgraph

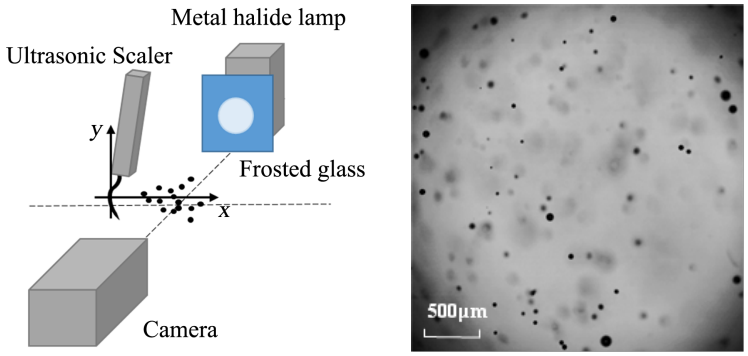


**Figure 3.** Schematic of the shadowgraph system. (a) Experimental setup;(b) Representative image.

measurement, and a metal halide lamp and frosted glass plate were installed opposite to the camera to obtain a uniform background light. The imaging area was 3 mm × 3 mm, and 3000 particle images were recorded at 60 fps. The countable number of droplets from these images was approximately 50,000 under typical conditions. A representative image of the droplets is shown in **Figure 3(b)**. The recorded images were preprocessed with median and Sobel filters, and only the focused droplets were evaluated. The droplet diameter and frequency were calculated after removing the droplets possessing an aspect ratio of 1.25 or higher to disregard the overlapped droplets. The droplet diameter was defined as the volume median diameter determined using the measured droplet size distribution.

The oscillation amplitude of the scaler tip in the horizontal direction ($x$) was measured to gain insights to the output characteristics of the dental ultrasonic scaler. The motion of the scaler tip was recorded using a high-speed camera (Photoron, FASTCAM Mini AX200, 1024 × 1024, 12 bits), and the distance moved was evaluated using the edge detection method. The recording frame rate was 360 kHz.

## 3. Results and Discussion

### 3.1. Oscillation of Ultrasonic Scaler

The motion of the ultrasonic scaler tip was analyzed using an edge-detection method to measure the oscillation amplitude. **Figure 4** shows the time series of the tip positions of the ultrasonic scaler with different output powers. The tip positions exhibited sinusoidal periodic oscillations. The frequencies of the oscillations are approximately 30 kHz at any output power. Only the oscillation amplitude $L_{pp}$ increased with an increase in the output power.

**Figure 5** shows the relationship between the output power of the ultrasonic scaler and the amplitude of oscillation of the scaler tip. The amplitude increased monotonically as the output power increased. In particular, the linear relationship between the output power and amplitude can be observed at output powers of 4 and above.

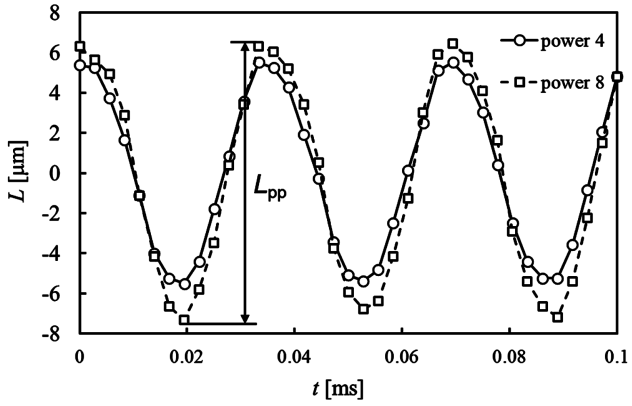


**Figure 4.** Time-series of tip positions.

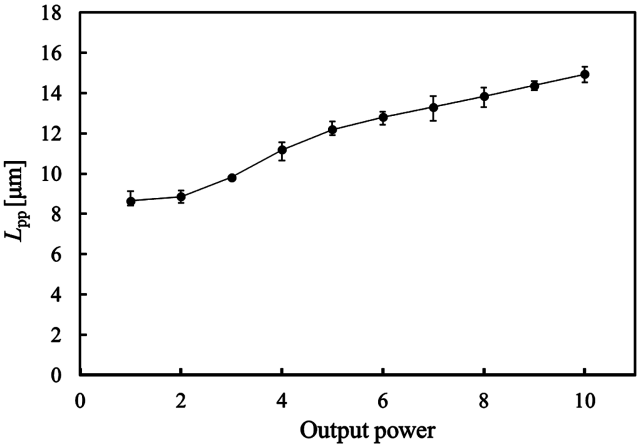


**Figure 5.** Oscillating amplitude.

### 3.2. Velocity Fields

**Figure 6** compares the velocity fields of the two-phase acoustic streaming at different oscillation amplitudes with a constant liquid flow rate of $Q_L$ = 0.38 mL/s. Acoustic streaming is generated horizontally at the curved part of the scaler tip and downward at the end of the scaler tip when the oscillation amplitude is small, as shown in **Figure 6(a)**. This is because the supplied liquid flows along the tip to the end of the scaler without detachment from the scaler tip owing to its weak oscillation. The maximum velocity was observed at a position away from the scaler tip in the flow generated at the curved part of the scaler tip. Acoustic streaming is generated horizontally only from the curved part of the scaler tip during a large oscillation, as shown in **Figure 6(b)**. The maximum velocity is increased by increasing the oscillation amplitude, which is detected at a position away from the scaler tip. This is caused by an increase in the acoustic energy emitted from the scaler tip.

**Figure 7** shows the variation in the maximum velocity magnitude of in-plane components and position of the acoustic streaming. The velocity measurements were conducted with output powers of 4, 6, 8, and 10. The maximum velocity increased slightly as the oscillation amplitude increased. The position of the

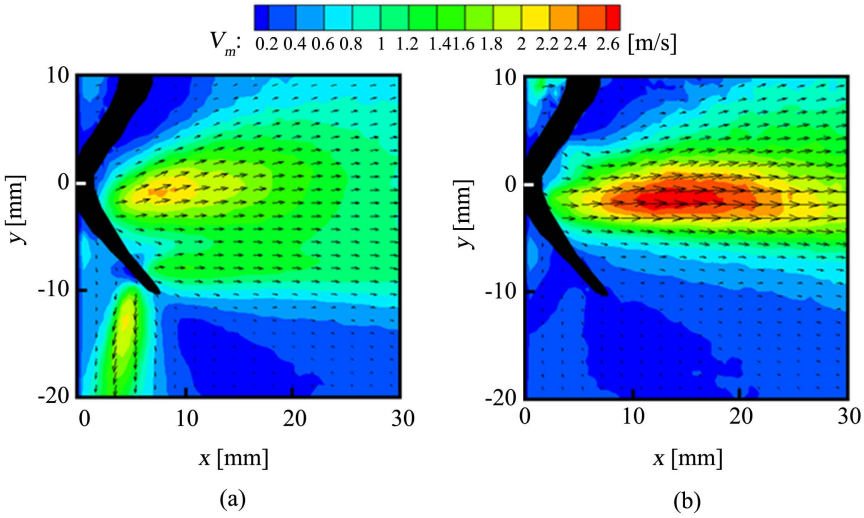


**Figure 6.** Mean velocity fields at a constant liquid flow rate ($Q_L$ = 0.38 mL/s). (a) Output power 4;(b) Output power 8.

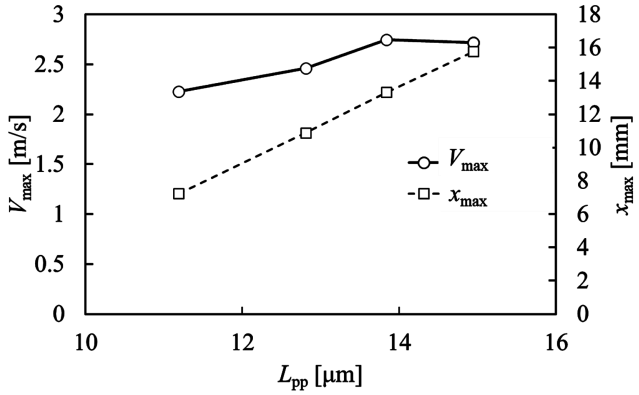


**Figure 7.** Variation of the maximum velocity with the oscillation of the ultrasonic scaler (Output powers of 4, 6, 8, and 10).

maximum velocity shifted in the downstream direction as the oscillation amplitude increased. The variation in the position of the maximum velocity is considered to be related to the acoustic focal region [13].

Figure 8 shows velocity fields of the acoustic streaming at different liquid flow rates. The output of the ultrasonic scaler is fixed at power 8. The flow field is reasonably stationary when no liquid is supplied to the scaler tip in Figure 8(a). This result implies that the velocity of the acoustic streaming of single-phase air is smaller than the measurable range of the present PIV. Moreover, this observation indicates that the effects of oil smoke, which was supplied for PIV, on the velocity field measurement and generation of the acoustic streaming are negligible. Because the supply of the oil smoke is much smaller than that of the cooling water due to the small particle diameter of the oil smoke. The acoustic flow is clearly observed when water is supplied in Figure 8(b) and Figure 8(c)). The acoustic streaming is generated from two positions: above the water supply hole as well as at the curved part of the scaler tip. The entire acoustic streaming is

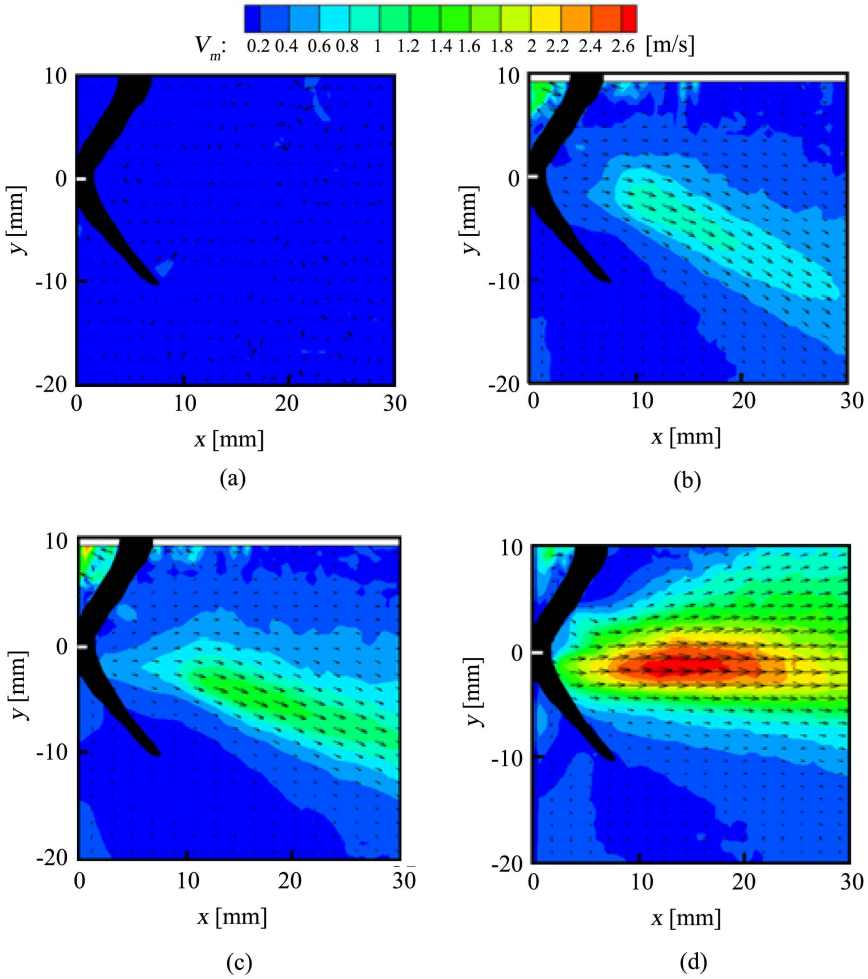


**Figure 8.** Mean velocity fields at a constant amplitude of the scaler oscillation (Output power 8). (a) $Q_L$ = 0 mL/s;(b) $Q_L$ = 0.07 mL/s;(c) $Q_L$ = 0.14 mL/s;(d) $Q_L$ = 0.38 mL/s.

directed downward owing to the influence on the downward acoustic streaming above the water supply port. The acoustic streaming from the curved position becomes dominant when the liquid flow rate increases further in **Figure 8(d)** and the entire stream flows in the horizontal direction. The variation in the direction of the acoustic streaming is expected to be combined influence of the gravity and the shape of the scaler tip. The maximum velocity increases as the liquid flow rate increases in the acoustic streaming.

**Figure 9** shows the variation in the maximum velocity magnitude of in-plane components with the liquid flow rate. The maximum velocity of single-phase acoustic streaming without liquid supply is extremely small. The maximum velocity increased when the flow rate of the supplied liquid increased. The change in the droplet velocity due to the flow rate has also been reported in the experiments of ultrasonic atomization [4], however, the mechanism has not been clarified. It is expected that the cavitational effects disturb the capillary waves [4] and liquid-droplet generation convert the acoustic energy into the flow more effectively [16]. In the present experiment, the change in the direction of the acoustic

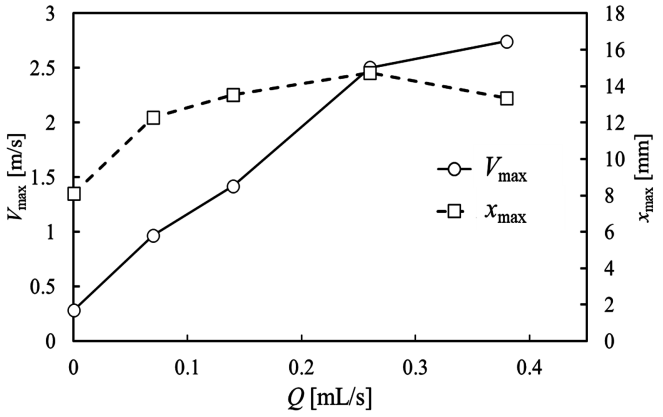


**Figure 9.** Variation of the maximum velocity with the liquid flow rate (Output power 8).

streaming was also observed as the flow rate increased. The variation in the direction of the acoustic streaming may be combined influence of the gravity and the shape on the surface of the scaler tip. The position of the maximum velocity occurred away from the scaler tip and changed slightly around $x = 14$ mm. This result implies the flow containing liquid droplets is accelerated by the acoustic energy.

### 3.3. Particle Property of Aerosol

The droplet diameter and appearance frequency of the droplet were measured to clarify the characteristics of the droplets generated by the ultrasonic scaler with a liquid flow rate of $Q_L = 0.38$ mL/s and output power 8. **Figure 10** shows a histogram of the particle size distributions at a typical distance from the scaler tip in the direction along the streaming ($y = 0$ mm). The $f$ of the droplets represents the appearance frequency with respect to the maximum of the total number of droplets among the experimental conditions. The measurable minimum diameter of the liquid droplet was 6 μm in this experiment. A peak was observed at a diameter of 25 μm near the scaler tip at $x = 20$ mm, and the diameter was distributed in the range of 10 - 100 μm. Some peaks in the histogram of the droplet size distribution may have been caused by a unique shape of the ultrasonic scaler tip. The distribution of the liquid droplet size was similar, but the appearance frequency decreased as the distance from the scaler tip increased. This result suggests that the liquid droplets generated by the vibration of the scaler tip are transported by acoustic streaming with less breakup and merging of liquid droplets.

**Figure 11** shows the variation in the droplet diameter with the distance from the scaler tip. The average droplet diameter was evaluated based on the droplet size distribution determined using the volume median diameter. The average droplet diameter was reasonably constant regardless of the distance from the nozzle and was approximately 40 μm. The relationship between the oscillation frequency $F$ and the diameter $d_p$ in ultrasonic atomization using the capillary wave is expressed using the Lang's empirical formula [2]:

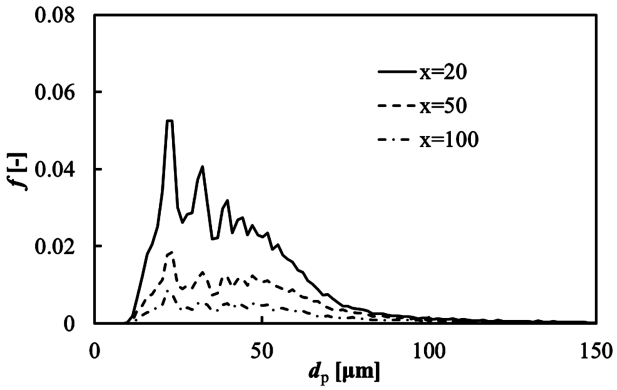


**Figure 10.** Histogram of particle size distribution (Output power 8, $Q_L$ = 0.38 mL/s).

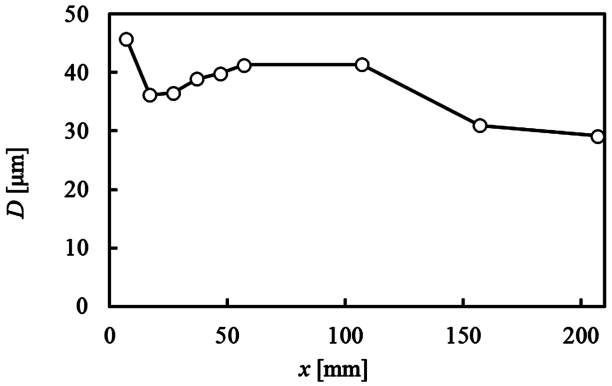


**Figure 11.** Variation of the average droplet diameter (Output power 8, $Q_L$ = 0.38 mL/s).

$$d_p = a\left(\frac{8\pi\gamma}{\rho F^2}\right)^{\frac{1}{3}} \tag{1}$$

where $a$ represents the empirical constant. $\gamma$ represents the surface tension, and $\rho$ represents the density of fluid. The empirical constant was $a$ = 0.34. Assuming that the water density and the surface tension are $\rho$ = 998 kg/m$^3$ and $\gamma$ = 72.88 × $10^{-3}$ N/m, respectively, the droplet diameter is $d_p$ = 43 μm. The predicted diameter is in good agreement with the results of the present experiment. Therefore, the Lang's empirical formula is applicable to droplets generated from an ultrasonic scaler.

## 4. Conclusion

In this study, velocity field and droplet diameter measurements were performed for a gas–liquid two-phase acoustic streaming generated from a dental ultrasonic scaler. The ultrasonic oscillation of the scaler tip led to the atomization of the cooling water and the subsequent generation of acoustic streaming. The acoustic streaming generated from the scaler tip increased as the oscillation amplitude increased and exhibited a maximum velocity at a region away from the scaler tip. The maximum velocity is significantly increased by the increase in the supplied flow rate, or the generated droplets. These droplets effectively enhanced the ve-

locity of the acoustic streaming in the two-phase case compared to the single-phase case without the droplets. The diameter of the generated droplets matched the diameter predicted from the oscillation frequency and they were transported by the acoustic streaming. These results suggested the importance of the droplets in the acoustic streaming of the ultrasonic scaler.

## Acknowledgements

This research was supported by a U-go grant from the Niigata University Research Administration Office.

## Conflicts of Interest

The authors declare no conflicts of interest regarding the publication of this paper.

## References

[1] Veena, H.R., Mahantesha, S., Joseph, P.A., Patil, S.R. and Patil, S.H. (2015) Dissemination of Aerosol and Splatter during Ultrasonic Scaling: A Pilot Study. *Journal of Infection and Public Health*, **8**, 260-265. https://doi.org/10.1016/j.jiph.2014.11.004

[2] Lang, R.J. (1962) Ultrasonic Atomization of Liquids. *The Journal of the Acoustical Society of America*, **34**, 6-8. https://doi.org/10.1121/1.1909020

[3] Avvaru, B., Patil, M.N., Gogate, P.R. and Pandit, A.B. (2006) Ultrasonic Atomization: Effect of Liquid Phase Properties. *Ultrasonics*, **44**, 146-158. https://doi.org/10.1016/j.ultras.2005.09.003

[4] Ramisetty, K.A., Pandit, A.B. and Gogate, P.R. (2013) Investigations into Ultrasound Induced Atomization. *Ultrasonics Sonochemistry*, **20**, 254-264. https://doi.org/10.1016/j.ultsonch.2012.05.001

[5] Boluriaan, S. and Morris, P.J. (2003) Acoustic Streaming: From Rayleigh to Today. *International Journal of Aeroacoustics*, **2**, 255-292. https://doi.org/10.1260/147547203322986142

[6] Eckart, C. (1948) Vortices and Streams Caused by Sound Waves. *Physical Review*, **73**, 68-75. https://doi.org/10.1103/PhysRev.73.68

[7] Suri, C., Takenaka, K., Yanagida, H., Kojima, Y. and Koyama, K. (2002) Chaotic Mixing Generated by Acoustic Streaming. *Ultrasonics*, **40**, 393-396. https://doi.org/10.1016/S0041-624X(02)00150-6

[8] Green, A., Marshall, J.S., Ma, D. and Wu, J. (2015) Acoustic Streaming, Fluid Mixing, and Particle Transport by a Gaussian Ultrasound Beam in a Cylindrical Container. *Physics of Fluids*, **27**, Article ID: 103601. https://doi.org/10.1063/1.4932232

[9] Tang, Q., Hu, J., Qian, S. and Zhang, X. (2017) Eckart Acoustic Streaming in a Heptagonal Chamber by Multiple Acoustic Transducers. *Microfluid Nanofluid*, **21**, Article No. 28. https://doi.org/10.1007/s10404-017-1871-1

[10] Naka, Y., Inoue, K. and Ishizaka, T. (2020) Development of an Ultrasound Acoustic Streaming Actuator for Flow Control. *Journal of Fluid Science and Technology*, **15**, JFST0003. https://doi.org/10.1299/jfst.2020jfst0003

[11] Kumar, A., Gogate, P.R. and Pandit, A.B. (2007) Mapping of Acoustic Streaming in Sonochemical Reactors. *Industrial & Engineering Chemistry Research*, **46**, 4368-4373.

https://doi.org/10.1021/ie060575q

[12] Schenker, M.C., Pourquié, M.J.B.M., Eskin, D.G. and Boersma, B.J. (2013) PIV Quantification of the Flow Induced by an Ultrasonic Horn and Numerical Modeling of the Flow and Related Processing Times. *Ultrasonics Sonochemistry*, **20**, 502-509. https://doi.org/10.1016/j.ultsonch.2012.04.014

[13] Hallez, L., Touyeras, F., Hihn, J.Y. and Bailly, Y. (2016) Characterization of HIFU Transducers Designed for Sonochemistry Application: Acoustic Streaming. *Ultrasonics Sonochemistry*, **29**, 420-427. https://doi.org/10.1016/j.ultsonch.2015.10.019

[14] Yamamoto, T., Kubo, K. and Komarov, S.V. (2021) Characterization of Acoustic Streaming in Water and Aluminum Melt during Ultrasonic Irradiation. *Ultrasonics Sonochemistry*, **71**, Article ID: 105381. https://doi.org/10.1016/j.ultsonch.2020.105381

[15] Fang, Y., Yamamoto, T. and Komarov, S. (2018) Cavitation and Acoustic Streaming Generated by Different Sonotorode Tips. *Ultrasonics Sonochemistry*, **48**, 79-87. https://doi.org/10.1016/j.ultsonch.2018.05.011

[16] Okabe, T., Sakamoto, S. and Watanabe, Y. (2001) Experimental Study on Acoustic Streaming in Water Containing Microcapsules. *Japanese Journal of Applied Physics*, **40**, 3861-3864. https://doi.org/10.1143/JJAP.40.3861

[17] Kiuchi, M., Fujisawa, N. and Tomimatsu, S. (2005) Performance of PIV System for Combusting Flow and Its Application to Spray Combustor Model. *Journal of Visualization*, **8**, 269-274. https://doi.org/10.1007/BF03181505

[18] Wieneke, B. (2015) PIV Uncertainty Quantification from Correlation Statistics. *Measurement Science and Technology*, **26**, Article ID: 074002. https://doi.org/10.1088/0957-0233/26/7/074002